

Diffusion-weighted MRI: a useful technique to discriminate benign versus malignant ovarian surface epithelial tumors with solid and cystic components

Wenhua Li,¹ Caiting Chu,¹ Yanfen Cui,¹ Ping Zhang,² Minjie Zhu³

¹Department of Radiology, Xinhua Hospital affiliated to Shanghai Jiao Tong University School of Medicine, 1665 KongJiang Road, Shanghai 200092, China

²Department of Obstetrics and Gynecology, Xinhua Hospital affiliated to Shanghai Jiao Tong University School of Medicine, 1665 Kong Jiang Road, Shanghai 200092, China

³Department of Pathology, Xinhua Hospital affiliated to Shanghai Jiao Tong University School of Medicine, 1665 Kong Jiang Road, Shanghai 200092, China

Abstract

Purpose: To evaluate differences in apparent diffusion coefficient (ADC) values for the solid component of benign and malignant ovarian surface epithelial tumors with the goal of differentiating benign versus malignant ovarian tumors preoperatively.

Materials and methods: A total of 127 patients with 131 pelvic masses identified by ultrasound between January 2006 and January 2011 were enrolled in this study. 46 patients were diagnosed with benign tumors, and 85 patients were diagnosed with malignant pathologies. For all of the patients, routine spin-echo MRI and diffusion-weighted imaging were performed. ADC values were determined for all of the masses, and the mean ADC values for the benign and malignant tumors were analyzed using Student's *t* test. A *P* value <0.05 was considered statistically significant.

Results: Mean ADC values associated with malignant ovarian surface epithelial tumors were significantly lower than the mean ADC values of the benign tumors. In addition, the range of ADC values associated with a 95% confidence interval did not overlap between the two groups. ROC analysis indicated that a cutoff ADC value of $1.25 \times 10^{-3} \text{ mm}^2/\text{s}$ was associated with 90.1% sensitivity and 89.9% specificity.

Conclusion: ADC values determined from 1.5 T MR DWI of benign and malignant ovarian masses were found to be significantly different.

Key words: Ovarian surface epithelial tumors—Magnetic resonance imaging—Apparent diffusion coefficient values—Benign—Malignant

Tumors deriving from ovarian surface epithelial cells account for 70%–75% of all ovarian neoplasms and are usually cystic and solid [1]. Despite the characterization of ovarian neoplasms by CA-125 serum levels, and imaging to determine tumor size, thickness of the walls and septa, as well as internal structures including papillary projections, nodularity, and the various degrees of solid components involved, determining the benign or malignant status of an ovarian neoplasm prior to surgery is usually not possible [2–5].

Diffusion-weighted magnetic resonance imaging (DW-MRI) is a technique that provides a non-invasive evaluation of the extent of microscopic diffusion present within biologic tissues. For example, DW-MRI can characterize tissues with respect to cell organization and density, microstructure, and microcirculation on the basis of the water diffusion properties associated with each of these aspects. Katayama et al. [6] previously evaluated the diagnostic performance of DW-MRI for the characterization of cystic ovarian tumors by determining apparent diffusion coefficient (ADC) values. However, the mean ADC values determined for the cystic components of malignant versus benign ovarian tumors showed no significant differences. Therefore, the purpose of this study

was to determine whether the ADC value that can be measured in the solid component within an ovarian tumor can facilitate the accurate diagnosis and differentiation of benign versus malignant lesions.

Materials and methods

Patients

This study was approved by our institutional committee and written informed consent was obtained from all subjects prior to the study. A total of 507 female patients evaluated for ovarian tumors between January 2006 and January 2011 were enrolled. Retrospective review of their MR imaging data was performed. The MR imaging studies of 127 patients with 131 ovarian epithelial tumors with solid component met the following criteria for inclusion in this study: (1) MR imaging was performed by using 1.5 T magnet, (2) both conventional MR imaging with dynamic contrast-enhancement and DW-MRI were performed, and the cases were proven by surgery-pathological examination. Of 507 patients, 87 were excluded for not having pelvic abnormality, 132 were excluded for not epithelial ovarian lesion including germ cell tumors ($n = 33$), sex cord stromal tumors ($n = 51$), and secondary ovarian lesions ($n = 48$). 161 were excluded for purely cystic ovarian lesions with thin and regular wall and/or septa.

MR protocol

All of the subjects underwent MRI by a 1.5 T MR unit (Twinspeed, GE Medical Systems, Milwaukee, WI, USA). The imaging protocol was comprised of axial non-contrast T1-weighted (TR/TE range, 400–600/10–14 ms) and axial T2-weighted (TR/TE range, 4000–6000/100–120 ms) imaging performed with a chemical shift-selective fat saturation pulse using the following parameters: slice thickness, 6 mm; gap, 1 mm; field of view (FOV), 32–42 cm; matrix, 256 × 256; and excitation, 2. Sagittal T1-weighted and T2-weighted (TR/TE range, 3000–6000/100–110 ms) fast spin-echo imaging without chemical shift-selective fat saturation pulse were also performed, as well as post-contrast enhanced axial and sagittal T1-weighted imaging using the same parameters described above except that a slice thickness of 5–7 mm was used. DW-MRI was acquired in the axial plane prior to administration of contrast medium by using a single-shot echo-planar imaging sequence (TR/TE effective range, 8000–10000/70–100; slice thickness, 6 mm; gap, 1 mm; FOV, 32–42 cm; matrix, 128 × 128; excitation, 2. b values of 0 and 1000 s/mm² were also applied in three orthogonal (Z, Y, and X) directions.

MR imaging analysis. Conventional MR data were analyzed in consensus on an Advantage Windows workstation 4.1 (GE Healthcare, Milwaukee, WI) by the two

radiologists (who had 15 and 10 years of experience in pelvic MR imaging, respectively) in two steps. In the first step, the readers reviewed the conventional MR images. In the second step, the readers reviewed the conventional and diffusion-weighted MR images. Tumors were classified into three types: (1) predominantly cystic (solid component less than one-third of tumor's volume), (2) mixed (solid component equal to one- to two-third of tumor's volume), (3) solid (solid component more than two-third of tumor's volume). The solid component according to a previously established classification by Timmerman et al. [7] included thickened septa, vegetation (papillary projection), and solid portions. The cystic component was defined as tissue that had homogeneous long T1 and T2 characteristics or different signal intensities on T1- or T2-weighted MR images and showed no enhancement after injection. The solid component, including papillary projections (vegetations), solid portions, and thickened septa, was defined as tissue that showed enhancement after injection. The signal intensity of solid components on T2-weighted MR images was defined as low or intermediate compared with that of the outer myometrium. The signal intensity of the cystic and solid components on DWI at $b = 1000$ s/mm² was classified as intermediate or low compared with that of serous fluid (urine or cerebrospinal fluid). The dynamic enhancement pattern of solid component according to a previously established type is judged to indicate persistent enhancement (type I), plateau (type II), and wash out (type III) [8]. The readers only characterized lesions as benign or malignant. The MR imaging criteria suggestive for benign were as follows: a purely unilocular or multilocular cystic lesions with a thin regular wall and septa, a regular and homogeneous solid component with low signal intensity on T2-weighted images, and a solid component with a type I enhancement pattern. The MR imaging criteria suggestive for malignant were considered as follows: papillary projections (vegetations), an irregular solid portion with intermediate signal intensity on T2-weighted images, and early uptake of contrast medium by a solid components, associated with a type III time-signal intensity curve, and the presence of ascites, peritoneal implants, and lymphadenopathy.

Data calculation and analysis

The cystic and solid components of the lesion were identified on T2-weighted and post-contrast T1-weighted images, and was matched on ADC maps. The ADC values of the solid and cystic components of each tumor were measured on DW images by a radiologist at an Advantage Windows workstation 4.1 (GE Healthcare, Milwaukee, WI), using the manufacturer's software (FuncTool; GE, Medical Systems). In order to minimize variability, the largest possible the regions of interest (ROIs), which varied from 15–90 mm², were manually

placed in the solid and cystic parts of the tumor. When the lesion exhibited a irregular or heterogeneous solid components, numerous vegetations or thickened irregular septa, 2–5 ROIs were drawn within the targeted components and the mean ADC value was used for the results.

Statistical analysis. The surgical pathological findings served as the reference standard for assessment of ovarian surface epithelial tumors. All of the analyses were performed using SPSS version 13.0 for Windows. Differences in mean tumor ADC values between benign and malignant groups were evaluated using Student's *t* test. A *P* value <0.05 was considered statistically significant. Receiver operating characteristic (ROC) curve analysis was performed to assess the diagnostic performance of the absolute ADC values in the characterization of benign versus malignant ovarian tumors.

Results

The final 127 patients with 131 lesions met our inclusion criteria. The mean age of the patients with benign versus malignant ovarian epithelial masses was 46.18 ± 15.52 and 59.88 ± 10.62 years, respectively. Forty-six (35.1%) of 131 tumors were benign: 26 serous cystadenomas, 16 mucinous cystadenomas, 3 serous cystadenofibromas, and 1 Brenner tumors. Eighty-five (64.9%) lesions were malignant: 33 serous cystadenocarcinomas, 25 mucinous cystadenocarcinomas, 12 borderline serous cystadenomas, 9 borderline mucinous cystadenomas, 3 endometrioid adenocarcinomas, 2 clear cell carcinomas, and 1 undifferentiated adenocarcinoma.

Conventional MR imaging findings according to histology is presented in Tables 1 and 2. The sensitivity, specificity, PPV (positive predictive value), NPV (negative predictive value), and accuracy of conventional MR imaging findings for predicting the nature of ovarian masses were 91.8% (78/85), 78.3% (36/46), 88.6% (78/88),

Table 2. Morphologic characteristics of 131 ovarian epithelial masses

MR imaging findings	Histology	
	Benign	Malignant
Predominantly cystic (<i>n</i> = 63)	36 (57.1%)	27 (42.9%)
Mixed (<i>n</i> = 47)	8 (17.0%)	39 (83.0%)
Solid (<i>n</i> = 21)	2 (9.5%)	19 (90.5%)

83.7% (36/43), and 87.0% (114/131). There was no difference in maximal diameter between benign and malignant masses. The presence of thickened or irregular septa was found in 63% of benign and 54.1% of malignant masses. Papillary projection or vegetation were less frequent in benign than in malignant masses (*P* < 0.001). Solid components were found in 11/46 benign and 37/85 malignant masses (*P* < 0.05). A lower incidence of low signal intensity within the solid component on T2-weighted images was found in malignant tumors (2 mucinous cystadenocarcinomas) than benign (3 serous cystadenofibromas, 1 Brenner tumors) in tumors (*P* < 0.005), Ascites were less frequently associated with benign masses and none of benign tumors was associated with peritoneal implants and lymphadenopathy.

DW imaging characterizations of the cystic and solid component of tumors were summarized in Table 3. The signal intensity within the cystic component at $b = 1000 \text{ s/mm}^2$ is approximately equal to that of serous fluid. The mean ADC value of the cystic component did not differ significantly between benign and malignant masses (*P* = 0.115). Among 46 benign tumors, 39 displayed intermediate signal intensity and 7 (3 mucinous cystadenomas, 3 serous cystadenofibromas, and 1 Brenner tumors) displayed low signal intensity of solid component at $b = 1000 \text{ s/mm}^2$ (Fig. 1). Among 85 malignant masses, only 2 (2 mucinous cystadenocarcinomas) showed low signal intensity and 83 displayed intermediate signal intensity of solid component at $b = 1000 \text{ s/mm}^2$ (Fig. 2). Mean ADC values of the

Table 1. The features of MR imaging findings

Characteristic	Benign (<i>n</i> = 46)	Malignant (<i>n</i> = 85)	<i>P</i> value
Mean lesion size (cm)	7.81	8.12	0.79
Thickened septa and/or wall	63.0% (29/46)	54.1% (46/85)	0.25
Vegetation	15.2% (7/46)	52.9% (45/85)	<0.001
Solid portion	23.9% (11/46)	43.5% (37/85)	0.03
Ascites	10.9% (5/46)	30.6% (26/85)	0.01
Peritoneal implants	0 (0/46)	14.1% (12/85)	0.005
Lymphadenopathy	0 (0/46)	15.3% (13/85)	0.005
Low T2 signal intensity	41.3% (19/46)	12.9% (11/85)	<0.001
Pattern of enhancement of the solid component			
Type I	76.1% (35/46)	13.4% (14/85)	0.001
Type II	23.9% (11/46)	22.4% (19/85)	0.98
Type III	0 (0/46)	61.2% (52/85)	0.001
Intensity on DW images within solid component at $b = 1000 \text{ s/mm}^2$			0.005
Low signal intensity	15.2% (7/46)	2.4% (2/85)	
Intermediate signal intensity	84.8% (39/46)	97.6% (83/85)	

Table 3. Patient characteristics associated with benign versus malignant ovarian lesions (unit $\times 10^{-3}$ mm²/s)

Characteristics	Benign		Malignant	
	Solid ADC	Cystic ADC	Solid ADC	Cystic ADC
Range of ADC values	1.25–2.13	2.21–3.09	0.66–1.31	1.79–2.91
Mean ADC values	1.69 \pm 0.25	2.58 \pm 0.27	1.03 \pm 0.22	2.44 \pm 0.33
95% confidence interval	1.58–1.80	2.48–2.68	0.95–1.12	2.32–2.56

tumor solid components were also determined for each of the groups, for the benign, the mean ADC value was $1.69 \times 10^{-3} \pm 0.25 \times 10^{-3}$ mm²/s (95% CI: 1.58 – 1.80×10^{-3} mm²/s), and for the malignant, the mean ADC value was $1.03 \times 10^{-3} \pm 0.22 \times 10^{-3}$ mm²/s (95% CI: 0.95 – 1.12×10^{-3} mm²/s). The lower ADC values associated with the malignant group were found to be statistically significant ($P < 0.01$).

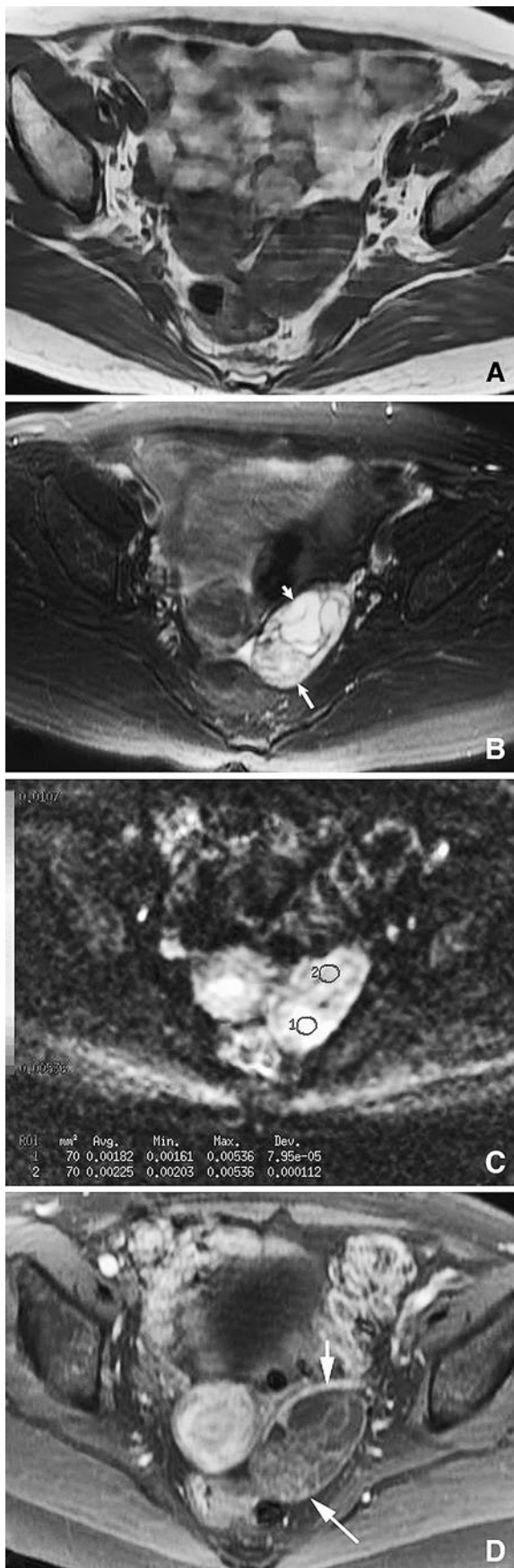
When the addition of DW imaging to conventional MR protocols, The sensitivity, specificity, PPV, NPV, and accuracy of conventional MR imaging findings for predicting the nature of ovarian masses were 96.5% (82/85), 89.1% (41/46), 94.3% (82/87), 93.2% (41/44), and 93.1% (122/131). It may increase the accuracy, sensitivity, specificity, PPV, and NPV of MR imaging distinguished benign and malignant ovarian epithelial tumors. Although there was some overlap associated with the absolute ADC values for the two groups, the 95% confidence limits did not have any overlap. Therefore, these preliminary results suggest that an ADC value $\geq 1.25 \times 10^{-3}$ mm²/s may be an optimal cutoff value for differentiating benign and borderline/malignant ovarian surface epithelial tumors. Furthermore, the sensitivity, specificity and area under curve associated with this cutoff value were 90.1% and 89.9%, and 0.91, respectively (Fig.3). Among them, only 7 benign lesions had ADC values lower than this cutoff value, and 2 of the borderline/malignant lesions had ADC values greater than this cutoff value. Based on these results, we hypothesize that this is a valid cutoff value for determining benign versus malignant ovarian surface epithelial tumors. However, additional studies of a larger number of cases will be needed to confirm these results.

Discussion

Currently, there is no gold standard for the diagnosis of a benign ovarian tumor versus a malignant ovarian tumor prior to surgery, especially when the tumor has both solid and cystic components. MR data that is used for the prediction of ovarian malignancies include lesion size (>6 cm), thickness of the walls and septa (>3 mm), and the detection of internal structures including papillary projections, nodularity, various degrees of solid components, necrosis, hemorrhage, or regions of striking enhancement following administration of contrast medium [6–10]. However, these imaging parameters have

been found to overlap for benign and malignant ovarian lesions. Therefore, as proposed by Katayama [6] and Thomassin-Naggara et al. [11], the abovementioned parameters are not always the most accurate predictors of ovarian malignancies. For example, in a recent series of 168 ovarian masses, papillary projections (vegetations) or nodularities were present in 37.5% of benign ovarian epithelial tumors. Further histological analysis demonstrated that these vegetations were present in 20%–26% of the benign tumor samples assayed, in 62%–78% of the borderline tumors assayed, and in 59%–92% of ovarian cancers assayed. Similarly, MRI detected vegetations present in 13%–22%, 61%–62%, and 38%–48% of benign, borderline, and invasive ovarian cancers, respectively [12]. Correspondingly, a diagnosis based on vegetation characteristics alone was associated with poor sensitivity and specificity. In the present study, lower mean ADC values were predominantly associated with malignant ovarian surface epithelial cystadenocarcinomas. Therefore, the addition of DW-MRI to routine MR pelvic protocols may increase the accuracy of distinguishing benign versus malignant ovarian pathologies.

It is well known that diffusion represents the thermally induced motion of molecules (Brownian motion). Within biological tissues, this microscopic motion includes the molecular diffusion of water, as well as the microcirculation of blood in the capillary networks. Furthermore, the rate of diffusion of water molecules in extracellular versus intracellular components of tissues has been shown to vary in vitro [6, 11, 13, 14]. For example, diffusion within the intracellular compartment can be relatively slow due to the presence of cellular membranes. Correspondingly, ADC values, which are quantitative expressions of the diffusion characteristics of tissues, are largely proportional to the ratio of extracellular and intracellular components. Therefore, ADC values tend to decrease with increased tissue cellularity or cell density. Accordingly, cell density can be representative of a tumor since intracellular organelles, matrix fibers, and soluble macromolecules can also contribute to diffusion restrictions. Thus, DW-MRI does not detect any restriction of water diffusion, or large ADC values, for healthy tissues, or for benign pathologic processes with a large extracellular space and little cellularity. However, when diffusion restrictions or small ADC values are detected, this may indicate a malignant tissue or the presence of hypercellularity. Therefore, DW-MRI,

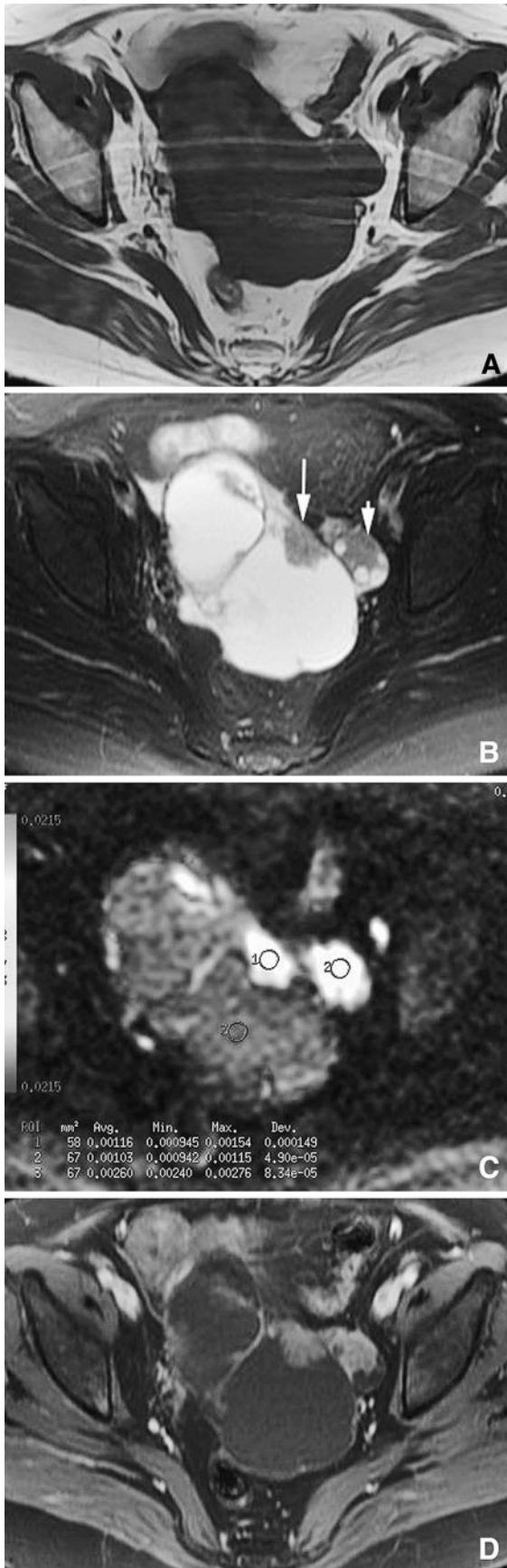


◀ **Fig. 1.** A 52-year-old woman with a cystadenoma. **A** Axial T1-weighted image shows a left ovarian mass with an isointensity. **B** Axial T2-weighted image reveals that the solid part of the ovarian mass is intermediate (*long arrow*) that is a malignant sign and the multiple cystic components is hyperintensity (*short arrow*). **C** Axial DWI shows the solid part of the mass is intermediate (*circle 1*, $ADC = 1.82 \times 10^{-3} \text{ mm}^2/\text{s}$); **D** Axial contrast-enhanced MR image shows a type I enhancement of the solid component.

and the corresponding measurements of ADC values, provides the optimal application of in vivo imaging methods for the quantification of capillary perfusion and water diffusion. While several authors have reported an association between decreased ADC values and various malignant tumors [13–16], the results of this study indicate there is a strong DWI signal that is associated with the solid portion of tumors, while the cystic portion produces a weaker signal. These results are consistent with previous characterizations of DWI signaling where stronger signals were found to be associated with increased cell density and low extracellular water content [15, 16].

In this study, DW-MRI with high b -values ($1000 \text{ s}/\text{mm}^2$) were associated with high levels of sensitivity (90.1%) and specificity (89.9%), and could differentiate benign ovarian tumors from malignant ovarian tumors. Additional advantages of using DW-MRI include that it is a non-invasive technique, it does not cause a patient significant discomfort, and it does not require exposure to ionizing radiation or injection of contrast materials. The results of this study also indicate that the addition of DW-MRI to conventional T1-weighted and T2-weighted MR protocols may increase the accuracy of distinguishing ovarian benign and malignant tumors using imaging, which could avoid the possible induction of fibrosis in patients with severe renal failure that would otherwise be effected by contrast material. Despite these advantages, there were also limitations associated with this preliminary study. For example, the population of patients evaluated was not very large. Therefore, our results will need to be confirmed in larger clinical studies. Second, this study only included cases of cystic and solid ovarian tumors, and not purely cystic tumors or tumors without solid masses. As a result, the observations made might not be directly applicable to all of the cases evaluated in the clinic. A continued evaluation of the clinical utility and indications of DW-MRI, therefore, still need to be investigated, especially since there are few reports regarding the use of ADC values for the differential diagnosis of ovarian tumors.

In conclusion, DW-MRI appears to be a useful method for differentiating benign epithelial ovarian tumors with solid components from malignant ovarian tumors, and is associated with a high sensitivity and



◀Fig. 2. A 51-year-old woman with bilateral ovarian cystadenocarcinomas. **A** An axial T1-weighted image of a pelvic mass with isointensity; **B** Axial T2-weighted image of a mass with an intermediate signal associated with a solid component (indicated with a *long arrow*) and a high signal associated with multiple cystic components present (indicated with a *short arrow*); **C** Axial DWI of high signals associated with a solid component (indicated with *long and short arrows*; *circle 1*, $ADC = 1.16 \times 10^{-3} \text{ mm}^2/\text{s}$; *circle 2*, $ADC = 1.03 \times 10^{-3} \text{ mm}^2/\text{s}$); **D** Axial contrast-enhanced MR image that shows a type III enhancement of a solid component.

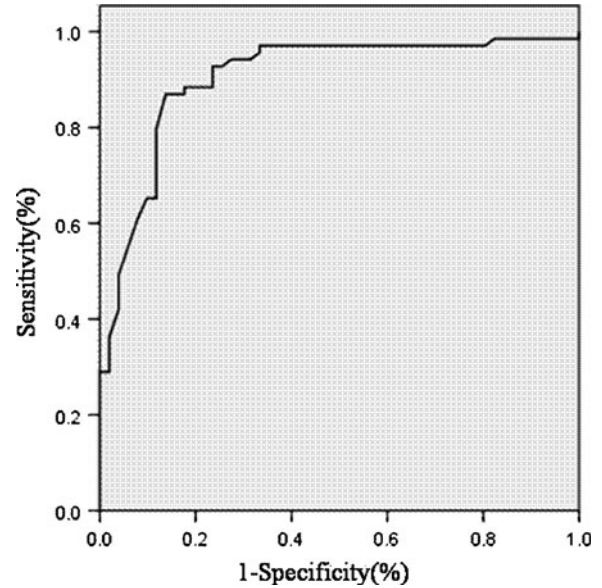


Fig. 3. ROC has largest area (0.91) under the curve and is probably best discriminator between benign and malignant ovarian masses when the absolute ADC value lower than $1.25 \times 10^{-3} \text{ mm}^2/\text{s}$.

specificity. A notable advantage of DW-MRI is also that it avoids the need for further injury of renal function due to an absence of contrast medium in this method. For patients with renal failure, this would prevent the development of fibrosis. Nevertheless, further studies with a larger number of cases are needed to support our findings.

References

1. Sutton CL, McKinney CD, Jones JE, Gay SB (1992) Ovarian masses revisited: radiologic and pathologic correlation. *Radiographics* 12:853–877
2. Bazot M, Darai E, Nassar-Slaba J, Lafont C, Thomassin-Naggara I (2008) Value of magnetic resonance imaging for the diagnosis of ovarian tumors: a review. *J Comput Assist Tomogr* 32:712–723
3. Sohaib SAA, Sahdev A, Trappen PV, Jacobs IJ, Reznek RH (2003) Characterization of adnexal mass lesions on MR imaging. *AJR* 180:1297–1304
4. Ghossain MA, Buy JN, Ligneres C, et al. (1991) Epithelial tumors of the ovary: comparison of MR and CT findings. *Radiology* 181:863–870

5. Jung SE, Lee JM, Rha SE, et al. (2002) CT and MR imaging of ovarian tumors with emphasis on differential diagnosis. *Radiographics* 22:1305–1325
6. Katayama M, Masui T, Kobayashi S, et al. (2002) Diffusion-weighted echo planar imaging of ovarian tumors: is it useful to measure apparent diffusion coefficients? *J Comput Assist Tomogr* 26:250–256
7. Timmerman D, Valentin L, Bourne TH, et al. (2000) Terms, definitions and measurements to describe the sonographic features of adnexal tumors: a consensus opinion from the International Ovarian Tumor Analysis(IOTA) Group. *Ultrasound Obstet Gynecol* 16:500–505
8. Thomassin-Naggara I, Darai E, Cuenod CA, et al. (2008) Dynamic contrast-enhanced magnetic resonance imaging: a useful tool for characterizing ovarian epithelial tumors. *J Magn Reson Imag* 28:111–120
9. Moteki T, Ishizaka H (1998) Evaluation of cystic ovarian lesions using apparent diffusion coefficient from turboFLASH MR images. *Br J Radiol* 71:612–620
10. Kim KA, Park CM, Lee JH, et al. (2004) Benign ovarian tumors with solid and cystic components that mimic malignancy. *AJR* 182:1259–1265
11. Thomassin-Naggara I, Darai E, Cuenod CA, et al. (2009) Contribution of diffusion-weighted MR imaging for predicting benignity of complex adnexal masses. *Eur Radiol* 19:1544–1552
12. Bazot M, Nassar-Slaba J, Thomassin-Naggara I, et al. (2006) MR imaging compared with intraoperative frozen-section examination for diagnosis of adnexal tumors; correlation with final histology. *Eur Radiol* 16:2687–2699
13. Umemoto M, Shiota M, Shimono T, et al. (2006) Preoperative diagnosis of ovarian tumors, focusing on the solid area based on diagnostic imaging. *J Obstet Gynaecol Res* 32:195–201
14. Thomassin-Naggara I, Toussaint I, Perrot N, et al. (2011) Characterization of complex adnexal masses: value of adding perfusion- and diffusion-weighted MR imaging to conventional MR imaging. *Radiology* 258:793–803
15. Erturk SM, Ichikawa T, Sano K, et al. (2008) Diffusion-weighted magnetic resonance imaging for characterization of focal liver masses: impact of parallel imaging (SENSE) and b value. *J Comput Assist Tomogr* 32:865–871
16. Nakai G, Matsuki M, Inada Y, et al. (2008) Detection and evaluation of pelvic lymph nodes in patients with gynecologic malignancies using body diffusion-weighted magnetic resonance imaging. *J Comput Assist Tomogr* 32:764–768